



Intravascular Ultrasound-Derived Virtual Fractional Flow Reserve for the Assessment of Myocardial Ischemia

Fumiyasu Seike, MD; Teruyoshi Uetani, MD; Kazuhisa Nishimura, MD; Hiroshi Kawakami, MD; Haruhiko Higashi, MD; Akira Fujii, MD; Jun Aono, MD; Takayuki Nagai, MD; Katsuji Inoue, MD; Jun Suzuki, MD; Shinji Inaba, MD; Takafumi Okura, MD; Kazunori Yasuda, PhD; Jitsuo Higaki, MD; Shuntaro Ikeda, MD

Background: Fractional flow reserve (FFR) is widely used for the assessment of myocardial ischemia. Intravascular ultrasound (IVUS) is an intracoronary imaging method that provides information about lumen and vessel morphology. Previous studies on the expanded use of IVUS to identify functional ischemia have noted an association between anatomy and physiology, but IVUS-derived minimum lumen area (MLA) has a weak-moderate correlation with myocardial ischemia compared with FFR. We developed a method to calculate FFR using IVUS-derived anatomical information for the assessment of myocardial ischemia. The aims of this study were to investigate the relationship between wire-based FFR and IVUS-derived FFR (IVUS-FFR) and to compare the usefulness of IVUS-FFR and IVUS-derived MLA for functional assessment.

Methods and Results: We retrospectively analyzed 50 lesions in 48 patients with coronary stenosis who underwent IVUS and FFR simultaneously. IVUS-FFR was calculated using our original algorithm and fluid dynamics. Mean percent diameter stenosis determined on quantitative coronary angiography and on FFR was 56.4 ± 10.7 and 0.69 ± 0.08 , respectively. IVUS-FFR had a stronger linear correlation with FFR ($R=0.78$, $P<0.001$; root mean square error, 0.057 FFR units) than with IVUS-derived MLA ($R=0.43$, $P=0.002$).

Conclusions: IVUS-FFR may be a more valuable method to identify myocardial ischemia, compared with IVUS-derived MLA.

Key Words: Fractional flow reserve; Intravascular ultrasound; Myocardial ischemia

The assessment of functional myocardial ischemia has an influence on the choice of management approach between medical therapy and revascularization.¹ Previous studies have shown that fractional flow reserve (FFR)-guided percutaneous coronary intervention (PCI) reduces major adverse cardiac events in patients with coronary artery disease (CAD).^{2–6} Intravascular ultrasound (IVUS) is an intracoronary imaging method that can provide information about lumen area, vessel area, and plaque burden that can be used for the guidance of PCI. Previous studies have investigated the expanded use of IVUS to identify hemodynamically severe stenosis, using FFR as a standard of reference.^{7–13} These studies noted an association between anatomy and physiology, but they suggested that minimum lumen area (MLA) has a weak-moderate correlation with myocardial ischemia. Fluid dynamics have proven to be the method of choice for obtaining accurate readings of flow in subject-specific

arterial geometries. We previously reported that optical coherence tomography (OCT)-derived FFR, which was calculated using a basic fluid dynamics equation, had a stronger correlation with FFR compared with conventional image-based measurements.¹⁴ We also developed a method to calculate IVUS-derived FFR (IVUS-FFR), which is calculated from an original fluid dynamics-based algorithm, for the assessment of myocardial ischemia. The aims of this study were to (1) investigate the relationship between wire-based FFR and IVUS-FFR; and (2) compare the usefulness of IVUS-FFR and IVUS-derived MLA for the functional assessment of CAD.

Methods

Study Design

Between April 2014 and June 2017, 57 lesions in 55 patients with stable angina pectoris were examined using both

Received September 23, 2017; revised manuscript received November 28, 2017; accepted December 4, 2017; released online January 25, 2018 Time for primary review: 29 days

Department of Cardiology, Pulmonology, Hypertension & Nephrology, Ehime University Graduate School of Medicine, Toon (F.S., T.U., K.N., H.K., H.H., A.F., J.A., T.N., K.I., J.S., T.O., J.H., S. Ikeda); Department of Cardiology, Kitaishikai Hospital, Ozu (S. Inaba); and Department of Mechanical Engineering, Ehime University Graduate School of Science and Engineering, Matsuyama (K.Y.), Japan

Mailing address: Fumiyasu Seike, MD, Department of Cardiology, Pulmonology, Hypertension & Nephrology, Ehime University Graduate School of Medicine, Shitsukawa, Toon 791-0295, Japan. E-mail: seike.fumiyasu.fx@ehime-u.ac.jp

ISSN-1346-9843 All rights are reserved to the Japanese Circulation Society. For permissions, please e-mail: cj@j-circ.or.jp

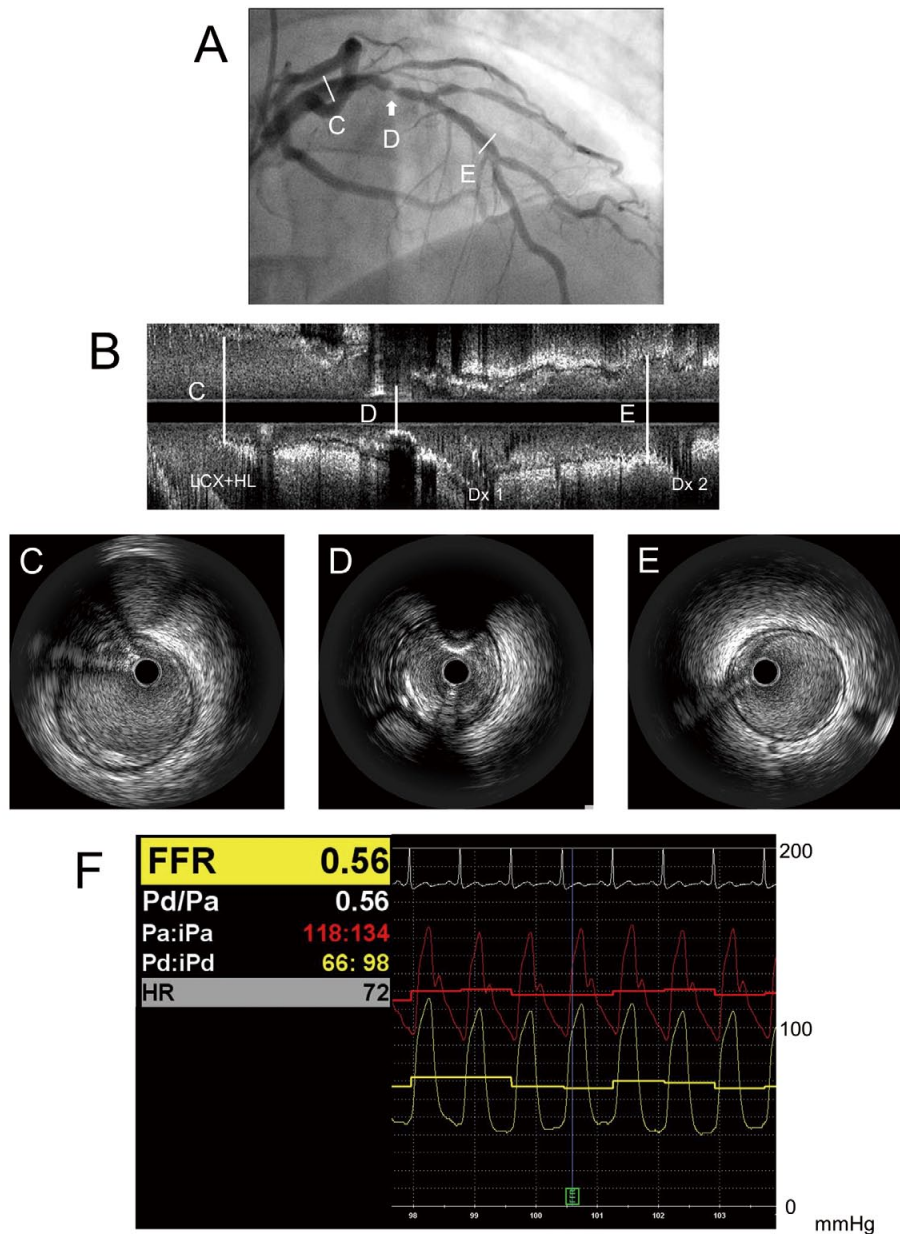


Figure 1. Coronary angiography, intravascular ultrasound (IVUS), and fractional flow reserve (FFR) in a representative case. **(A)** Coronary angiogram showing severe stenosis at the proximal portion of the left anterior descending coronary artery. **(B)** Longitudinal IVUS showing severe stenosis **(D)** at the proximal portion of the left anterior descending coronary artery. **(C)** Proximal reference lumen area was 14.98 mm². **(D)** Minimum lumen area was 2.07 mm². **(E)** Distal reference lumen area was 10.78 mm². **(F)** FFR. Pressure loss (ΔP) was calculated from the equation $\Delta P = FV + SV^2$, where F is the coefficient of pressure loss due to viscous friction (Poiseuille resistance), and S is the coefficient of local pressure loss due to abrupt enhancement (flow separation), and F and S were calculated from IVUS data. V is coronary flow velocity. F was calculated as the sum of each longitudinal 1-mm slice on IVUS. In this case, F was calculated as 0.142 mmHg s/cm. S was calculated using the largest area of the analyzed segment and minimum lumen area. In this case, S was calculated as 0.0153 mmHg s²/cm². The stenotic flow reserve (SFR) was calculated using the following formulas: $P = 100 - (FV + SV^2)$, $P = 10 + V \times (100 - 10) / 4.2$. The intersection point of both formulas was defined as SFR **(Figure 2)**. In this case, SFR was calculated as 2.33. The pressure loss of the lesion was calculated using the formula $FV + SV^2$. The pressure loss of the diastolic phase was calculated as follows: $0.142 \times (20 \times 2.33) + 0.0153 \times (20 \times 2.33)^2 = 39.8$ mmHg. The pressure loss of the systolic phase was calculated as follows: $0.142 \times (10 \times 2.33) + 0.0153 \times (10 \times 2.33)^2 = 11.6$ mmHg.

$$\frac{(60 - 39.8) \times \frac{2}{3} + (120 - 11.6) \times \frac{1}{3}}{80} = 0.620$$
. Therefore, IVUS-FFR was calculated as 0.620. The wire-based FFR was 0.56.

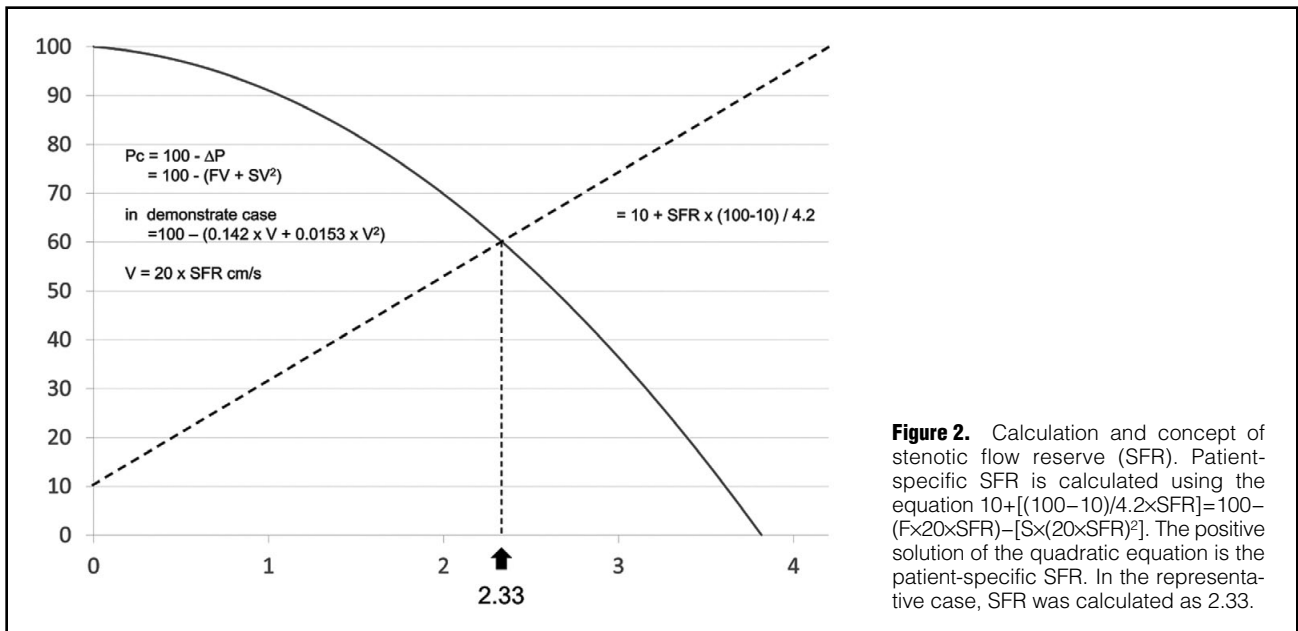


Figure 2. Calculation and concept of stenotic flow reserve (SFR). Patient-specific SFR is calculated using the equation $10 + [(100 - 10) / 4.2 \times \text{SFR}] = 100 - (F \times 20 \times \text{SFR}) - [S \times (20 \times \text{SFR})^2]$. The positive solution of the quadratic equation is the patient-specific SFR. In the representative case, SFR was calculated as 2.33.

IVUS and FFR for the assessment of myocardial ischemia at Ehime University Graduate School of Medicine. Patients who had severe left ventricular (LV) hypertrophy, hypertrophic cardiomyopathy, severe systolic dysfunction, an infarct-related artery, significant valvular disease, left main trunk-left anterior descending coronary artery or left main trunk-left circumflex coronary artery true bifurcation lesion in addition to a history of PCI in the target vessel, lesion length >60 mm in the left coronary artery, target vessel implanted with ≥ 2 stents, or severe respiratory disease with home oxygen therapy were excluded from the present study. Seven lesions (7 patients) were excluded due to meeting the exclusion criteria. The present institutional review board approved the retrospective use of patient data for this study (Institutional Review Board of Ehime University Hospital, approval no. 1606007). The requirement for informed consent was waived due to the retrospective nature of the study. Patient records and information were anonymized and de-identified prior to analysis.

Coronary Angiography and FFR

Coronary angiography was performed using 6- or 7-Fr coronary catheters. Intracoronary isosorbide dinitrate was given before angiography, IVUS, and advancement of the pressure-monitoring guidewire (Verrata, Phillips, MA, USA, or AERIS, Abbott, CA, USA) into the distal coronary vessel past the lesion. The visual severity of coronary artery stenosis was evaluated based on the American Heart Association classification system.

FFR was performed before any intervention took place. Hyperemia was induced by i.v. adenosine triphosphate at a rate of 0.16 mg/kg/min as previously reported.¹⁵

Quantitative coronary angiography analysis was performed offline by an experienced analyst, who was blinded to the IVUS and FFR results, using CAAS II (Pie Medical Imaging BV, Netherlands). After selection of the optimal projection displaying the most severe stenosis, percent diameter stenosis (%DS) at end-diastole, minimum lumen diameter, reference vessel diameter, and lesion length were measured.

IVUS

IVUS analysis was performed with a validated quantitative IVUS analysis system (VISIATLAS, Terumo, Tokyo, Japan) by an experienced investigator, blinded to clinical information except coronary angiography data. An IVUS lesion was defined as >0.5-mm atherosclerotic plaque thickness.¹⁶

Gray-scale IVUS and ultrasound signals were acquired with a commercially available IVUS imaging system (VISIWAVE, Terumo) using a 43-MHz mechanically rotating IVUS catheter (View IT, Terumo). IVUS was performed using motorized pullback at 0.5 mm/s to include proximal and distal Luer connectors. Quantitative IVUS measurements for each frame (median interslice distance, 1.0 mm) included external elastic membrane (EEM), lumen, and plaque and media (EEM minus lumen) cross-sectional area, plaque burden (plaque and media divided by EEM), and MLA. Area stenosis was calculated by the following formula: $1 - (\text{MLA} / \text{proximal reference lumen cross-sectional area})$. Volumes were calculated using Simpson's rule and reported as normalized area (volume divided by length). The plaque burden (%) was calculated as the TPV/total vessel volume $\times 100$. The percentage of lipid area and the percentage of fibrous area at each slice were automatically calculated using the integrated backscatter (IB)-IVUS system. The total lipid volume (TLV) and total fibrous volume (TFV) were also calculated using Simpson's method. The percentage of TLV and the percentage of TFV were calculated according to the following formulas: $\text{TLV} / \text{TPV} \times 100$, $\text{TFV} / \text{TPV} \times 100$. The percent change in each volume was calculated as: $(\text{volume at follow-up} - \text{volume at baseline}) / \text{volume at baseline} \times 100$.¹⁷

IVUS-FFR

IVUS-FFR was determined using our original algorithm, which was developed with the Fluid Dynamics Laboratory at Ehime University. Gould et al have shown that the calculated pressure loss (ΔP) across an area of stenosis can be described by the following simplified equation: $\Delta P = FV + SV^2$.¹⁸

Table 1. Baseline Clinical Patient and Lesion Characteristics

Patient characteristics		n=48
Age (years)		69.0±9.6
Men		40 (83)
Height (cm)		163.2±9.5
Body weight (kg)		63.7±12.2
BMI (kg/m ²)		23.8±3.4
Hypertension		36 (75)
Dyslipidemia		34 (71)
Current smoker		17 (35)
Diabetes mellitus		26 (54)
Previous MI		6 (13)
Previous PCI		19 (40)
Previous CABG		0
Lesion characteristics		n=50
Index coronary artery		
Left main trunk		2 (4)
Left anterior descending		32 (64)
Left circumflex		7 (14)
Right		9 (18)
AHA classification type B2+C		24 (48)

Data given as mean ± SD or n (%). AHA, American Heart Association; BMI, body mass index; CABG, coronary artery bypass grafting; MI, myocardial infarction; PCI, percutaneous coronary intervention.

$$\Delta P = \frac{8\pi\mu L}{A_s} \frac{A_n}{A_s} \times V + \frac{k}{2} \left(\frac{A_n}{A_s} - 1 \right)^2 \times V^2,$$

$$F = \frac{8\pi\mu L}{A_s} \frac{A_n}{A_s}, \quad S = \frac{\rho}{2} \left(\frac{A_n}{A_s} - 1 \right)^2$$

where μ is absolute blood viscosity, L is stenosis length, A_n is cross-sectional area of the normal artery (reference lumen area), A_s is cross-sectional area of the stenosis segment, V is flow velocity, ρ is blood density, k is a constant related to entrance and exit effects here equal to 1, and F and S are the coefficients of pressure loss due to viscous friction and exit separation. Resistance was calculated from IVUS geometry for both Poiseuille resistance due to viscous friction (F), assuming laminar flow in the converging portion of the stenosis, and for resistance due to exit separation (S) due to vortex formation in the diverging portion of the stenosis. In this study, the coefficients were described as $\mu=4.0 \times 10^{-3} \text{ Pa} \cdot \text{s}$, and $\rho=1,050 \text{ kg/m}^3$. These were calculated using IVUS measurements L , A_n , and A_s .

The coefficients F and S were determined by the morphology of the coronary stenosis (length, axial and cross-sectional shapes, diameter of the normal artery, and minimum cross-sectional area of the stenosis).¹⁹ Longitudinal length per frame of IVUS was 1 mm. The sum of resistance of all of the frames was equivalent to the Poiseuille resistance of the entire lesion. Coefficient S was calculated using the MLA and the larger area of the proximal or distal reference area. A representative case and calculation are shown in **Figure 1**.

We calculated IVUS-FFR using stenotic flow reserve (SFR). Assuming a mean arterial pressure of 100 mmHg, the coronary flow can increase to 5- or 4.2-fold its value at rest without stenosis.^{18,20–23} In this study, maximum SFR was determined as 4.2. Patient-specific SFR was calculated

by the following equation (**Figure 2**): $P_c=100-\Delta P=100-(FV+SV^2)$, where P_c (coronary pressure distal to the stenosis) is defined as the translesional pressure. In **Figure 2**, P_c is plotted on the vertical axis, and coronary artery velocity (V) is plotted on the horizontal axis as a ratio of velocity at hyperemia to velocity at normal flow at rest ($V_{\text{hyperemia}}/V_{\text{rest}}=\text{SFR}$). In the SFR calculation, coronary flow velocity=0.2 m/s results in SFR=1, and coronary flow velocity=0.4 m/s produces SFR=2. The dotted line plots the relationship between coronary perfusion pressure and coronary flow under conditions of maximum coronary vasodilation in the presence of a stenosis, as previously documented experimentally,²¹ according to the equation: $10+[(100-10)/4.2 \times \text{SFR}]$. The solid line is a plot of the relation between P_c and flow in the presence of a stenosis. This solid line is the graphic plot of the equation at the bottom of the figure derived from the equation: $100-\Delta P=100-(FV+SV^2)$. The intersection of the curve with the line representing coronary perfusion pressure under hyperemia is the patient-specific SFR.

In the representative case, SFR was calculated to be 2.33 (**Figure 1**). It is important that we use basal coronary flow velocity (0.2 m/s) only for SFR calculation, as explained in previous studies.^{21,23} Details of the calculation conditions are described in the Appendix. For the next calculation, we use coronary and phase-specific velocities.

According to previous reports, basal (diastolic/systolic) left coronary artery flow was determined as (20/10) cm/s, and basal (diastolic/systolic) right coronary artery flow was determined as (15/10) cm/s using our algorithm.²⁴ Diastolic phase pressure loss (diastolic ΔP) is calculated using the following equation: $[F \times (\text{basal coronary flow velocity} \times \text{SFR})] + [S \times (\text{basal coronary flow velocity} \times \text{SFR})^2]$. Systolic phase pressure loss (systolic ΔP) is calculated by the following equation: $[F \times (\text{basal coronary flow velocity} \times \text{SFR})] + [S \times (\text{basal coronary flow velocity} \times \text{SFR})^2]$.

In this study, we assumed the systolic/diastolic (mean) blood pressure to be 120/60 (80) mmHg based on previous studies.^{15,25}

Diastolic-phase pressure is calculated using the following equation: $60 - (\text{diastolic } \Delta P)$. Systolic phase pressure is calculated using the following equation: $120 - (\text{systolic } \Delta P)$. The proportion of diastolic time was determined as 2/3 of the complete cardiac cycle. Finally, IVUS-FFR was calculated using the following equation:

$$\frac{(60 - \text{diastolic } \Delta P) \times \frac{2}{3} + (120 - \text{systolic } \Delta P) \times \frac{1}{3}}{80} = \text{IVUS - FFR value}$$

Statistical Analysis

Statistical analysis was performed using SPSS version 18.0 (IBM, Armonk, NY, USA). Categorical variables are summarized as n (%). Continuous variables are presented as mean ± SD. Linear regression analysis was performed to determine the correlation between wire-based FFR and IVUS-FFR. Bland-Altman analysis was performed to compare the measurements of wire-based FFR and IVUS-FFR. $P < 0.05$ was considered to indicate statistical significance.

Results

Baseline clinical and lesion characteristics are listed in

Table 2. Correlation of Coronary Angiography and IVUS for FFR			
		R	P-value
QCA			
Diameter stenosis (%)	56.4±10.7	-0.427	0.002
Minimum lumen diameter (mm)	1.10±0.33	0.281	0.048
Reference vessel diameter (mm)	2.56±0.60	-0.072	0.621
Lesion length (mm)	26.8±18.3	0.027	0.854
IVUS analysis at MLA site			
Lumen CSA (mm ²)	1.74±0.65	0.428	0.002
EEM CSA (mm ²)	11.0±4.4	0.122	0.452
Area stenosis (%)	73.9±17.7	-0.470	0.001
Plaque burden (%)	83.0±5.8	-0.344	0.015
Proximal reference lumen CSA (mm²)	8.07±3.39	-0.308	0.030
IVUS volumetric analysis			
Lesion length (mm)	34.2±17.7	-0.174	0.228
Mean EEM CSA (mm ³ /mm)	12.2±4.4	-0.013	0.927
Mean lumen CSA (mm ³ /mm)	4.8±1.8	-0.013	0.929
Plaque burden (%)	59.9±8.7	-0.099	0.495
IVUS-FFR parameters			
Coefficient of f (s/cm×10 ⁻¹)	2.10±1.29	-0.382	0.006
Coefficient of s (s ² /cm ² ×10 ⁻³)	9.47±8.43	-0.546	<0.001
Stenotic flow reserve	2.66±0.47	0.680	<0.001
IVUS-derived pressure loss (mmHg)	24.2±7.3	-0.685	<0.001
IVUS-FFR	0.703±0.088	0.781	<0.001
FFR measurements			
FFR	0.689±0.077		
FFR ≤0.8	49 (98)		
Wire-based pressure loss (mmHg)	26.0±8.7		
Mean aortic pressure (mmHg)	84.0±14.1		
Wire-based mean translesional pressure (mmHg)	58.0±11.0		
IVUS evaluations			
Max calcification arc (°)	195±131	0.005	0.972
Attenuated plaque	27 (54)		0.949
IB-IVUS at MLA site			
Calcium (%)	2.9±2.9	0.211	0.141
Dens fibrosis (%)	7.0±4.0	0.15	0.298
Fibrosis (%)	34.6±9.8	-0.199	0.165
Lipid (%)	55.5±13.1	0.057	0.693
IB-IVUS volumetric analysis			
Calcium (%)	2.5±1.9	0.077	0.593
Dens fibrosis (%)	6.7±3.5	0.063	0.666
Fibrosis (%)	39.7±8.5	-0.116	0.424
Lipid (%)	51.1±12.4	0.049	0.735

Data given as mean ± SD or n (%). CSA, cross-sectional area; EEM, external elastic membrane; FFR, fractional flow reserve; IB, integrated backscatter; IVUS, intravascular ultrasound; MLA, minimum lumen area; QCA, quantitative coronary angiography.

Table 1. Mean patient age was 69.0±9.6 years, and 83% were male. The correlations of quantitative coronary angiography and IVUS parameters with wire-based FFR are listed in **Table 2**. On quantitative angiographic analysis, the mean stenosis diameter and minimum lumen diameter were 56.4±10.7% and 1.10±0.33 mm, respectively. Mean IVUS-derived MLA, percent area stenosis (%AS), IVUS-FFR and wire-based FFR were 1.74±0.65 mm², 73.9±17.7, 0.703±0.088, and 0.689±0.077, respectively. IVUS-FFR showed a stronger linear correlation with wire-based FFR (R=0.781, P<0.001; root mean square error=0.057 FFR units, **Figure 3A**) than with quantitative

coronary angiography -%DS (R=-0.427, P=0.002), IVUS measurements of MLA (R=0.428, P=0.002, **Figure 3B**), and %AS (R=-0.470, P=0.001, **Figure 3D**). Only IVUS-FFR had a strong correlation with wire-based FFR (**Figure 4**). There was no significant correlation between plaque characteristics and FFR (**Table 2**).

Discussion

The major findings of this study are as follows: IVUS-FFR was strongly correlated with wire-based FFR, while IVUS and angiographic anatomical measurements, including

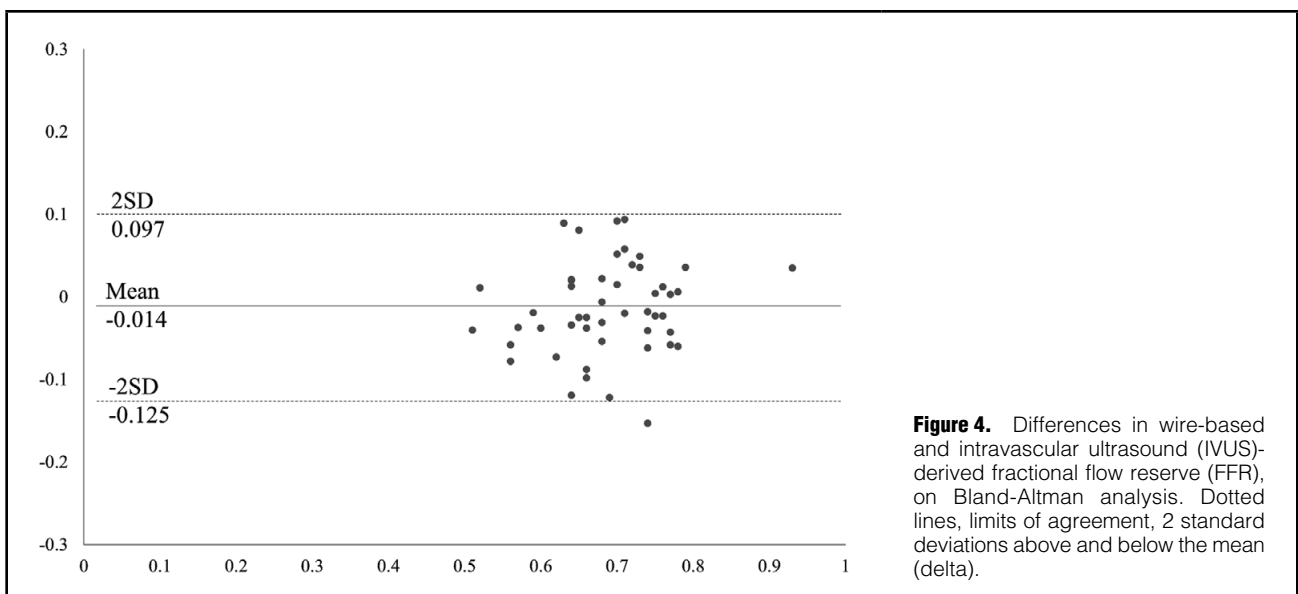
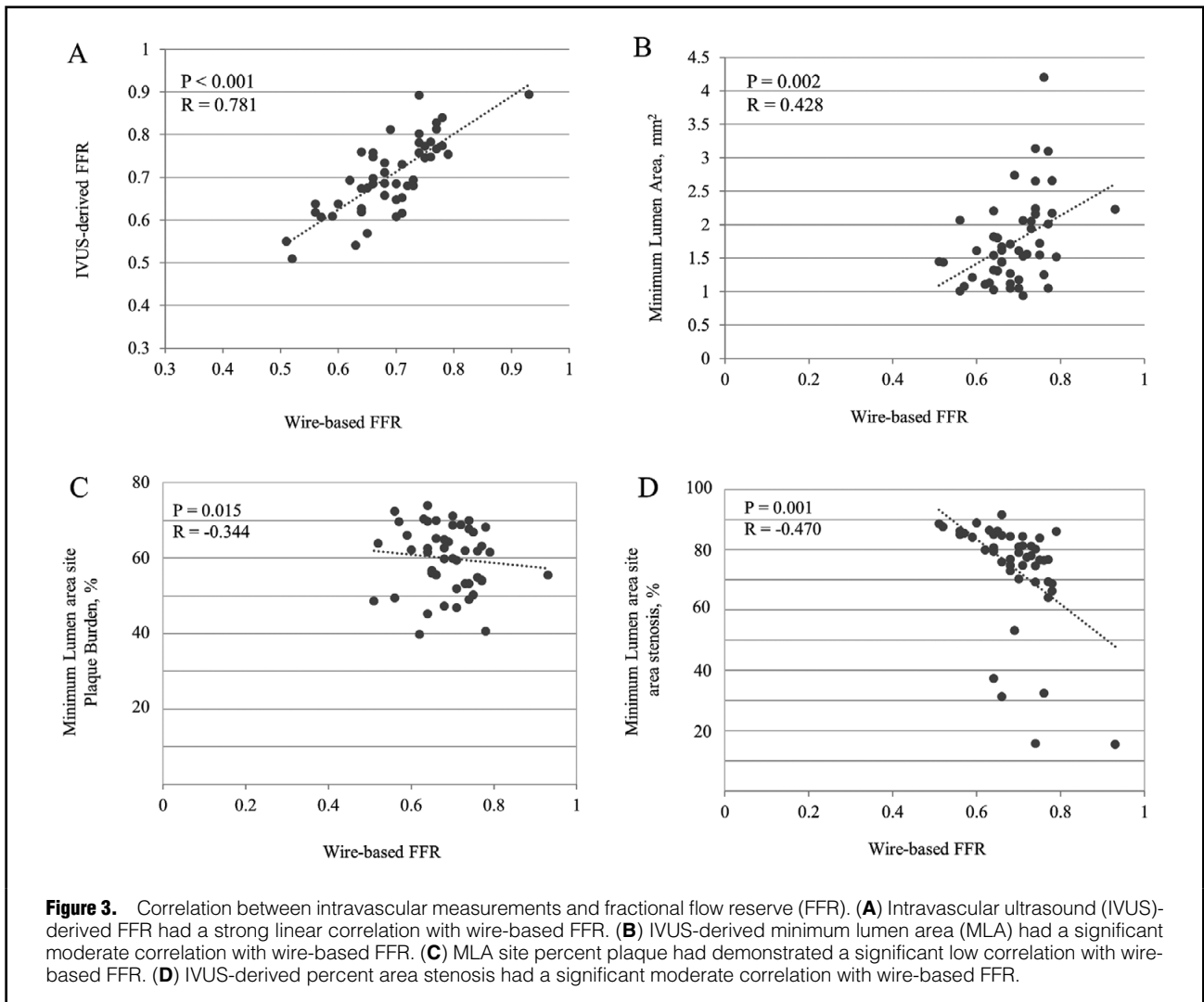


Table 3. Calculation of MLA Using IVUS for Myocardial Ischemia

Study	Year	n	Against	Imaging modality	Cut-off MLA (mm ²)	R	Sensitivity (%)	Specificity (%)	Accuracy (%)
Nishioka et al ²⁶	<i>J Am Coll Cardiol</i> , 1999	70	SPECT	IVUS	4.0	–	88	90	–
Takagi et al ⁷	<i>Circulation</i> , 1999	51	0.75	IVUS	3.0	0.786	83.0	92.3	–
Briguori et al ⁸	<i>Am J Cardiol</i> , 2001	53	0.75	IVUS	4.0	0.41	92	56	79
Ben-Dor et al ⁹	<i>EuroIntervention</i> , 2011	92	0.80	IVUS	3.2	0.34	69.2	68.3	70
Kang et al ¹⁰	<i>Circ Cardiovasc Interv</i> , 2011	236	0.80	IVUS	2.4	0.507	90	60	68
Kang et al ¹¹	<i>Am J Cardiol</i> , 2012	784	0.80	IVUS	2.4	0.481	83.2	62.6	68.5
Koo et al ¹²	<i>JACC Cardiovasc Interv</i> , 2011	267	0.80	IVUS	2.75	–	69	65	67
Gonzalo et al ²⁷	<i>J Am Coll Cardiol</i> , 2012	47	0.80	IVUS	2.36	0.141	67	65	66
Waksman et al ¹³	<i>J Am Coll Cardiol</i> , 2013	367	0.80	IVUS	3.07	0.55	64.0	64.9	–

SPECT, single-photon emission computed tomography. Other abbreviations as in Table 2.

Table 4. Calculation of FFR Using Intracoronary Imaging

Study	Year	Method	Imaging modality	R
IVUS-FFR	Present study	Basic fluid dynamics	IVUS	0.78
Seike et al (our method) ¹⁴	<i>Am J Cardiol</i> , 2017	Basic fluid dynamics	OCT	0.89
Ha et al ³³	<i>Circ Cardiovasc Interv</i> , 2016	CFD	OCT	0.72
Guagliumi et al ³²	<i>Eurointervention</i> , 2013	Vascular resistance ratio	OCT	0.81
Zafar et al ³¹	<i>Int Heart J</i> , 2014	Blood flow resistance model	OCT	0.69

CFD, computational fluid dynamics; OCT, optical coherence tomography. Other abbreviations as in Table 2.

IVUS-derived MLA, had weak-moderate linear correlations with FFR, consistent with previous studies. Therefore, IVUS-FFR may provide useful diagnostic information that can predict functional ischemia based on wire-based FFR.

Over the past 20 years, there has been an ongoing discussion of the differences between anatomical and functional assessment of coronary stenosis. This debate has extended to intracoronary imaging techniques. IVUS studies, however, have demonstrated mild-moderate correlations between structural severity and functional severity using MLA. Takagi et al first reported that IVUS-derived MLA ≤ 3.0 mm² predicted FFR ≤ 0.75 in 42 patients.⁷ Briguori et al also evaluated 53 intermediate lesions, and suggested that IVUS-derived MLA ≤ 4.0 mm² had a sensitivity of 92% and specificity of 56% for detecting FFR ≤ 0.75 .⁸ Previous reports using IVUS-derived MLA to assess myocardial ischemia are summarized in **Table 3**.^{7–13,26,27} The accuracy of IVUS-derived MLA to identify functional ischemia ranged from 66% to 79%. Thus, IVUS-derived MLA is limited in accuracy. Moreover, the MLA cut-offs for myocardial ischemia were 2.36–4.0 mm², representing a very wide cut-off range. MLA, which is a single cross-sectional area of a vessel, is only one of many factors influencing flow, and it does not reflect the amount of myocardium. Therefore, previous studies attempted to determine the cut-off based on reference vessel diameter.^{11,13} Flow separation, known as Bernoulli's principle, can be calculated using MLA and reference vessel diameter. Although this method represents an improvement over the

use of MLA alone, it does not consider lesion longitudinal structure, which also affects myocardial ischemia. Therefore, we think that myocardial ischemia cannot be accurately measured using only reference vessel diameter and MLA. We previously reported that OCT-derived FFR, which was calculated using fluid dynamics, was strongly correlated with wire-based FFR.¹⁴ In the present study, IVUS-FFR, which reflects not only MLA and reference vessel diameter but also longitudinal structure, also had a good correlation with wire-based FFR. Many studies have reported the existence of lesions with anatomical and physiological mismatch.²⁸ It is possible that there is no way to accurately evaluate anatomical severity. IVUS-FFR is a relatively simple technique that can accurately evaluate the anatomical severity of coronary lesions, and therefore it is expected to help clarify the detailed association and true frequency of mismatch between anatomy and physiology.

Coronary computed tomography (CT) angiography-derived FFR, which is based on computational fluid dynamics, can predict myocardial ischemia accurately,^{29,30} and is an excellent method for detecting myocardial ischemia. CT angiography-derived FFR, however, has some limitations. A difference in error of 600 μ m on CT greatly affects the calculation of FFR, and calcified lesions are difficult to analyze with coronary CT.²³ IVUS is superior to CT in spatial resolution and can accurately measure any type of lesion. CT angiography-derived FFR also requires high computing capacity and a long calculation time. Furthermore, 3-D reconstruction of the coronary artery requires extremely high skill, knowledge, and time. In

contrast, our method uses basic fluid dynamics and does not require a high-performance computer. Therefore, IVUS-FFR is easy to determine and the calculation time is short. Therefore, we believe that IVUS-FFR will be useful in daily catheter laboratory practice.

Previously published papers that calculated FFR using intravascular imaging are summarized in **Table 4**.^{14,31–33} We were unable to find any previous studies that reported the calculation of FFR using IVUS. Compared with previous methods, IVUS-FFR produced similar results. In addition, the IVUS-FFR technique reported here is the only FFR calculation method to use IVUS. Zafar et al and Guagliumi et al reported that accurate volumetric measurement of the lumen profile with OCT correlates closely with FFR.^{31,32} These methods calculate the resistance of each coronary lesion. Ha et al reported that OCT-derived FFR, which depends on computational fluid dynamics, could accurately predict myocardial ischemia, and suggested that computational fluid dynamics might enable the assessment of functional information.³³ Although computational fluid dynamics is a useful method to calculate FFR, it requires a high-performance computer, long calculation time, and strict 3-D reconstruction of the coronary arteries. Therefore, FFR may be difficult to calculate in catheter laboratories in daily practice using computational fluid dynamics. In the near future, the adoption of 60-MHz IVUS systems in daily practice is becoming increasingly widespread, and automated lumen tracing methods are expected to improve. Therefore, IVUS-FFR may become a routine method in catheter laboratories.

Study Limitations

This study had several limitations. First, this retrospective study included a relatively small number of discrete coronary lesions. Given, however, that almost all exclusions were made on the basis of less reliable IVUS measurements, selection bias is unlikely. Despite the small sample size, a good correlation was seen between the IVUS-FFR and FFR measurements. Second, our algorithm assumed several parameters. Third, the present study did not consider the influence of side branches. Flow rate is difficult to calculate for bifurcation lesions. Flow rate has an effect on pressure loss. Guagliumi et al reported that accurate volumetric measurement of the lumen profile with OCT correlates closely with FFR.³² It is difficult, however, to render all lumen borders in a clinical situation in daily practice. Therefore, we constructed a simple algorithm for IVUS-FFR. Fourth, IVUS-FFR could not evaluate the effect of curvature. There was no information about curvature of the coronary artery on IVUS. And fifth, this study did not include patients with severe LV hypertrophy, hypertrophic cardiomyopathy, severe systolic dysfunction, an infarct-related artery, or significant valvular disease, because these disorders might influence coronary circulation. In the present study IVUS-FFR was calculated based on normal coronary circulation. Therefore, to precisely evaluate patients with these disorders, further investigation is needed.

Conclusions

IVUS-FFR, which was calculated using an original fluid dynamics-based algorithm, was more strongly correlated with wire-based FFR than MLA. IVUS-FFR may provide useful information for the assessment of myocardial

ischemia, and this novel algorithm may help to clarify the true association between anatomy and physiology in patients with CAD.

Acknowledgments

We are grateful to Motosuke Sogo for writing the IVUS-FFR calculation algorithm.

Funding Sources

This work was supported by JSPS KAKENHI Grant Number 10771561.

Disclosures

J.H. received research grants from Abbott Vascular Japan. The other authors declare no conflicts of interest.

References

- Escaned J, Banning A, Farooq V, Echavarria-Pinto M, Onuma Y, Ryan N, et al. Rationale and design of the SYNTAX II trial evaluating the short to long-term outcomes of state-of-the-art percutaneous coronary revascularisation in patients with de novo three-vessel disease. *EuroIntervention* 2016; **12**: e224–e234.
- Tonino PA, De Bruyne B, Pijls NH, Siebert U, Ikeno F, van't Veer M, et al. Fractional flow reserve versus angiography for guiding percutaneous coronary intervention. *N Engl J Med* 2009; **360**: 213–224.
- De Bruyne B, Pijls NH, Kalesan B, Barbato E, Tonino PA, Piroth Z, et al. Fractional flow reserve-guided PCI versus medical therapy in stable coronary disease. *N Engl J Med* 2012; **367**: 991–1001.
- De Backer O, Biasco L, Lonborg J, Pedersen F, Holmvang L, Kelbaek H, et al. Long-term outcome of FFR-guided PCI for stable coronary artery disease in daily clinical practice: A propensity score-matched landmark analysis. *EuroIntervention* 2016; **11**: e1257–e1266.
- Tanaka H, Chikamori T, Tanaka N, Hida S, Igarashi Y, Yamashita J, et al. Diagnostic performance of a novel cadmium-zinc-telluride gamma camera system assessed using fractional flow reserve. *Circ J* 2014; **78**: 2727–2734.
- Shiono Y, Kubo T, Tanaka A, Ino Y, Yamaguchi T, Tanimoto T, et al. Long-term outcome after deferral of revascularization in patients with intermediate coronary stenosis and gray-zone fractional flow reserve. *Circ J* 2015; **79**: 91–95.
- Takagi A, Tsurumi Y, Ishii Y, Suzuki K, Kawana M, Kasanuki H. Clinical potential of intravascular ultrasound for physiological assessment of coronary stenosis: Relationship between quantitative ultrasound tomography and pressure-derived fractional flow reserve. *Circulation* 1999; **100**: 250–255.
- Briguori C, Anzuini A, Airolidi F, Gimelli G, Nishida T, Adamian M, et al. Intravascular ultrasound criteria for the assessment of the functional significance of intermediate coronary artery stenoses and comparison with fractional flow reserve. *Am J Cardiol* 2001; **87**: 136–141.
- Ben-Dor I, Torguson R, Gaglia MA Jr, Gonzalez MA, Maluenda G, Bui AB, et al. Correlation between fractional flow reserve and intravascular ultrasound lumen area in intermediate coronary artery stenosis. *EuroIntervention* 2011; **7**: 225–233.
- Kang SJ, Lee JY, Ahn JM, Mintz GS, Kim WJ, Park DW, et al. Validation of intravascular ultrasound-derived parameters with fractional flow reserve for assessment of coronary stenosis severity. *Circ Cardiovasc Interv* 2011; **4**: 65–71.
- Kang SJ, Ahn JM, Song H, Kim WJ, Lee JY, Park DW, et al. Usefulness of minimal luminal coronary area determined by intravascular ultrasound to predict functional significance in stable and unstable angina pectoris. *Am J Cardiol* 2012; **109**: 947–953.
- Koo BK, Yang HM, Doh JH, Choe H, Lee SY, Yoon CH, et al. Optimal intravascular ultrasound criteria and their accuracy for defining the functional significance of intermediate coronary stenoses of different locations. *JACC Cardiovasc Interv* 2011; **4**: 803–811.
- Waksman R, Legutko J, Singh J, Orlando Q, Marso S, Schloss T, et al. FIRST: Fractional flow reserve and intravascular ultrasound relationship study. *J Am Coll Cardiol* 2013; **61**: 917–923.
- Seike F, Uetani T, Nishimura K, Kawakami H, Higashi H, Aono J, et al. Intracoronary optical coherence tomography-derived

- virtual fractional flow reserve for the assessment of coronary artery disease. *Am J Cardiol* 2017; **120**: 1772–1779.
15. Miyagawa M, Kumano S, Sekiya M, Watanabe K, Akutzu H, Imachi T, et al. Thallium-201 myocardial tomography with intravenous infusion of adenosine triphosphate in diagnosis of coronary artery disease. *J Am Coll Cardiol* 1995; **26**: 1196–1201.
 16. Kapadia SR, Nissen SE, Ziada KM, Guetta V, Crowe TD, Hobbs RE, et al. Development of transplantation vasculopathy and progression of donor-transmitted atherosclerosis: Comparison by serial intravascular ultrasound imaging. *Circulation* 1998; **98**: 2672–2678.
 17. Inaba S, Okayama H, Funada J, Higashi H, Saito M, Yoshii T, et al. Impact of type 2 diabetes on serial changes in tissue characteristics of coronary plaques: An integrated backscatter intravascular ultrasound analysis. *Eur Heart J Cardiovasc Imaging* 2012; **13**: 717–723.
 18. Gould KL, Kelley KO, Bolson EL. Experimental validation of quantitative coronary arteriography for determining pressure-flow characteristics of coronary stenosis. *Circulation* 1982; **66**: 930–937.
 19. Tron C, Kern MJ, Donohue TJ, Bach RG, Aguirre FV, Caracciolo EA, et al. Comparison of quantitative angiographically derived and measured translesion pressure and flow velocity in coronary artery disease. *Am J Cardiol* 1995; **75**: 111–117.
 20. Seike F, Uetani T, Nishimura K, Iio C, Kawakami H, Fujimoto K, et al. Correlation between quantitative angiography-derived translesional pressure and fractional flow reserve. *Am J Cardiol* 2016; **118**: 1158–1163.
 21. Kirkeeide RL, Gould KL, Parsel L. Assessment of coronary stenoses by myocardial perfusion imaging during pharmacologic coronary vasodilation. VII. Validation of coronary flow reserve as a single integrated functional measure of stenosis severity reflecting all its geometric dimensions. *J Am Coll Cardiol* 1986; **7**: 103–113.
 22. Pijls NH, van Son JA, Kirkeeide RL, De Bruyne B, Gould KL. Experimental basis of determining maximum coronary, myocardial, and collateral blood flow by pressure measurements for assessing functional stenosis severity before and after percutaneous transluminal coronary angioplasty. *Circulation* 1993; **87**: 1354–1367.
 23. Johnson NP, Kirkeeide RL, Gould KL. Coronary anatomy to predict physiology: Fundamental limits. *Circ Cardiovasc Imaging* 2013; **6**: 817–832.
 24. Wieneke H, Haude M, Ge J, Altmann C, Kaiser S, Baumgart D, et al. Corrected coronary flow velocity reserve: A new concept for assessing coronary perfusion. *J Am Coll Cardiol* 2000; **35**: 1713–1720.
 25. Leppo JA. Comparison of pharmacologic stress agents. *J Nucl Cardiol* 1996; **3**: S22–S26.
 26. Nishioka T, Amanullah AM, Luo H, Berglund H, Kim CJ, Nagai T, et al. Clinical validation of intravascular ultrasound imaging for assessment of coronary stenosis severity: Comparison with stress myocardial perfusion imaging. *J Am Coll Cardiol* 1999; **33**: 1870–1878.
 27. Gonzalo N, Escaned J, Alfonso F, Nolte C, Rodriguez V, Jimenez-Quevedo P, et al. Morphometric assessment of coronary stenosis relevance with optical coherence tomography: A comparison with fractional flow reserve and intravascular ultrasound. *J Am Coll Cardiol* 2012; **59**: 1080–1089.
 28. Park SJ, Kang SJ, Ahn JM, Shim EB, Kim YT, Yun SC, et al. Visual-functional mismatch between coronary angiography and fractional flow reserve. *JACC Cardiovasc Interv* 2012; **5**: 1029–1036.
 29. Norgaard BL, Leipsic J, Koo BK, Zarins CK, Jensen JM, Sand NP, et al. Coronary computed tomography angiography derived fractional flow reserve and plaque stress. *Curr Cardiovasc Imaging Rep* 2016; **9**: 2.
 30. Min JK, Taylor CA, Achenbach S, Koo BK, Leipsic J, Norgaard BL, et al. Noninvasive fractional flow reserve derived from coronary CT angiography: Clinical data and scientific principles. *JACC Cardiovasc Imaging* 2015; **8**: 1209–1222.
 31. Zafar H, Sharif F, Leahy MJ. Feasibility of intracoronary frequency domain optical coherence tomography derived fractional flow reserve for the assessment of coronary artery stenosis. *Int Heart J* 2014; **55**: 307–311.
 32. Guagliumi G, Sirbu V, Petroff C, Capodanno D, Musumeci G, Yamamoto H, et al. Volumetric assessment of lesion severity with optical coherence tomography: Relationship with fractional flow. *EuroIntervention* 2013; **8**: 1172–1181.
 33. Ha J, Kim JS, Lim J, Kim G, Lee S, Lee JS, et al. Assessing computational fractional flow reserve from optical coherence tomography in patients with intermediate coronary stenosis in the left anterior descending artery. *Circ Cardiovasc Interv* 2016; **9**: e003613.